Research paper

Synthesis, crystal structure, cytotoxicity study, DNA / protein binding and molecular docking of dinuclear copper(II) complexes

Apurba Bhunia, Soumen Mistri, Rajesh Kumar Manne, Manas Kumar Santra, Subal Chandra Manna

PII: S0020-1693(18)31761-4
DOI: https://doi.org/10.1016/j.ica.2019.03.022
Reference: ICA 18827

To appear in: *Inorganica Chimica Acta*

Received Date: 21 November 2018
Revised Date: 15 March 2019
Accepted Date: 15 March 2019

Please cite this article as: A. Bhunia, S. Mistri, R.K. Manne, M.K. Santra, S.C. Manna, Synthesis, crystal structure, cytotoxicity study, DNA / protein binding and molecular docking of dinuclear copper(II) complexes, *Inorganica Chimica Acta* (2019), doi: https://doi.org/10.1016/j.ica.2019.03.022

Synthesis, crystal structure, cytotoxicity study, DNA / protein binding and molecular docking of dinuclear copper(II) complexes

Apurba Bhunia,[a] Soumen Mistri,[a] Rajesh Kumar Manne,[b] Manas Kumar Santra,[b] and Subal Chandra Manna*,[a]

[a]*Department of Chemistry and Chemical Technology, Vidyasagar University, Midnapore 721102, West Bengal, India, E-mail: scmanna@mail.vidyasagar.ac.in, Fax: (91) (03222) 275329.*

[b]*National Centre for Cell Science, NCCS Complex, Pune University Campus Ganeshkhind, Pune-411 007, Maharashtra, India*

Abstract

The Schiff base 2-[(3-Methylamino-propylimino)-methyl]-phenol (HL) has been used for the synthesis of three dinuclear Cu(II) complexes, namely $[Cu_2L_2(dca)_2]$ (**1**), $[Cu_2L_2(2,5\text{-}pdc)_2]\cdot 6H_2O$ (**2**), $[Cu_2L_2(tp)]$ (**3**), where dca= dicyanamide, 2,5-pdc= pyridine-2,5-dicarboxylate and tp= terephthalate. In **2**, HL acts as bidentate (O, N) chelating ligand, while tridentate (O, N, N) in **1** and **3**. In all the complexes copper(II) is in its five coordination with distorted trigonal bipyramidal geometry in **1**, whereas distorted square pyramidal in **2** and **3**. Non covalent interactions give rise supramolecular architectures in all complexes. Cytotoxicity of the complexes was examined using breast cell lines MCF7 and MDA-MB-231. Complexes **1** and **2** show dose dependent suppression of MCF7 and MDA-MB- 231 cells and the related IC_{50} values are 26 ± 2.9 μM and 51 ± 4.7 μM for MCF7 cell, 16.4 ± 1.6 μM and 43.2 ± 3.1 μM for MDA-MB- 231 cell. Interaction of complexes **1**-**3** with bovine serum albumin (BSA), human serum albumin (HSA) and calf thymus DNA have been studied by electronic absorption and fluorescence spectroscopic technique. Molecular docking study has been used to explain the interaction of complexes with serum albumins.

Keywords: Dinuclear Cu(II) complex; Cytotoxicity study; DNA binding; Serum albumin binding; Molecular docking

Introduction

The most efficient and widely used approach for design and synthesis of coordination compounds is the self-assembly of metal ions and ligands [1]. Schiff bases are most useful ligands in the chemistry of 3d metal coordination compounds. Pseudo-halides and organic carboxylates are good co-ligands to coordinate with metal sites. Transition metal Schiff base compounds are important for their biological activity [2]. In addition to well known platinum anticancer compounds, a good number of studies have been performed on transition metal complexes for their ability to destroy cancer cells [3]. In comparison with other 3d metal complexes, Cu(II) complexes are more suitable due to their less toxicity and important cellular effects such as neurotransmission, cellular respiration, etc.[4]. Literature study reveals that several synthetic Cu(II) complexes act as potential anticancer and cancer inhibiting agents, and some of them have been found to be active both in vitro and in vivo [4]. On the other hand bovine serum albumin and human serum albumin are most important protein in blood plasma and they transport and distribute various endogenous and exogenous substances, like nutriments, medicines, etc. Transportation and distribution of drugs depend on the interaction of drugs with serum albumin (SA) molecules [5]. Moreover many Cu(II) complexes have been observed to exhibit enhanced DNA binding and cleavage activities [6]. Therefore study of the kinetics of interaction of CT-DNA/serum albumin are important for the development of Cu(II) Schiff base based metallo-pharmaceuticals.

2-[(3-Methylamino-propylimino)-methyl]-phenol (HL) is a potential flexidentate chelating ligand. Using this ligand and in combination with azide, three copper(II) complexes namely $[Cu_2L_2(N_3)_2]$, $[Cu_2L_2(N_3)_2]\cdot H_2O$ and $[CuL(N_3)]_n$ have been reported in the literature where the ligand HL acts as N,N,O donor tridentate chelating ligand [7]. The Cu(II) centres in all these three reported complexes possess five-coordinate square pyramidal geometries. However till now there is no report on coppe(II) complexes of this ligand in combination with dicarboxylate and dicyanamide. In the present contribution we have used HL in combination with dicarboxylate / dicyanamide, and synthesized complexes $[Cu_2L_2(dca)_2]$ (**1**), $[Cu_2L_2(2,5\text{-pdc})_2]\cdot 6H_2O$ (**2**) and $[Cu_2L_2(tp)]$ (**3**) (where dca= dicyanamide, 2,5-pdc= pyridine-2,5-dicarboxylate and tp= terephthalate). DNA/protein binding activities have been studied. Anticancer activities in human breast cancer cell lines MCF7 and MDA-MB-231 have been investigated.

Experimental

Chemicals and instrumentation

N-methyl-1,3-diaminopropane and sodium dicyanamide were purchased from Sigma Aldrich Chemical Company and all other chemical were of AR grade. Solvents used were purified by standard methods [8].

Elemental analyses were performed using a Perkin-Elmer 240C elemental analyzer. ^{1}HNMR spectra of ligand recorded in $CDCl_3$ on 400 MHz instrument. IR spectra were recorded as KBr pellets on a Bruker Vector 22 FT IR spectrophotometer. ESI-MS spectra were obtained from ESI mass spectrometry. UV-Vis spectra in room temperature were recorded on Shimadzu UV-1601 UV-vis spectrophotometer. Emission spectra were recorded on a Hitachi F-7000 spectrofluorimeter. Quantum yield was calculated according to the reported method,[9] where phenol in water medium used as reference.

Synthesis of the ligand

The ligands 2-[(3-Methylamino-propylimino)-methyl]-phenol (HL) was prepared by condensation of N-methyl-1,3-diaminopropane and 2-hydroxybenzaldehydein methanol at room temperature.

A methanolic solution (10 ml) of N-methyl-1,3-diaminopropane (10 mmol, 0.882 g) was added drop wise to a methanolic solution (10 ml) of 2-hydroxybenzaldehyde (10 mmol, 1.22 g) with constant stirring. Resulting yellow reaction mixture was stirred for 3 h. The yellow color compound was separated using column chromatographic technique using 1:1 ethyl acetate and hexane solvent and the compound was characterized adopting FT-IR, ^{1}H NMR and mass spectrometry techniques. Yield: 1.57g (82 %). $C_{11}H_{16}N_2O$ (192.25): C, 68.72; H, 8.38; N, 14.57%. Found: C, 68.71; H, 8.37; N, 14.58 (%). IR (KBr), cm^{-1}: 3200-3600 (br, vs), 2982 (s), 2943 (s), 1641 (vs), 1550 (vs), 1466 (s), 1413 (vs), 1372 (s), 1300 (s), 1281 (w), 1160 (w), 1112 (w), 1076 (s) 882 (w), 819 (w), 781 (w), 671 (s) 629 (s) 564 (w). ^{1}H NMR ($CDCl_3$, 400 MHz, δ, ppm): 8.22 s (1H), 7.09-7.02 d (2H), 6.99-6.92 t (2H), 4.14 s (1H), 3.09-3.01 m (1H), 2.74-2.6 m (6H), 2.59-2.5 d (3H). MS (in MeOH, calcd m/z): 192.2511 ($C_{11}H_{16}N_2O$), 177.1124 ($C_{10}H_{13}N_2O$), 133.1394 (C_8H_7NO).

Synthesis of the Complexes

Synthesis of complexes **1**-**3** are schematically displayed in Scheme **1**.

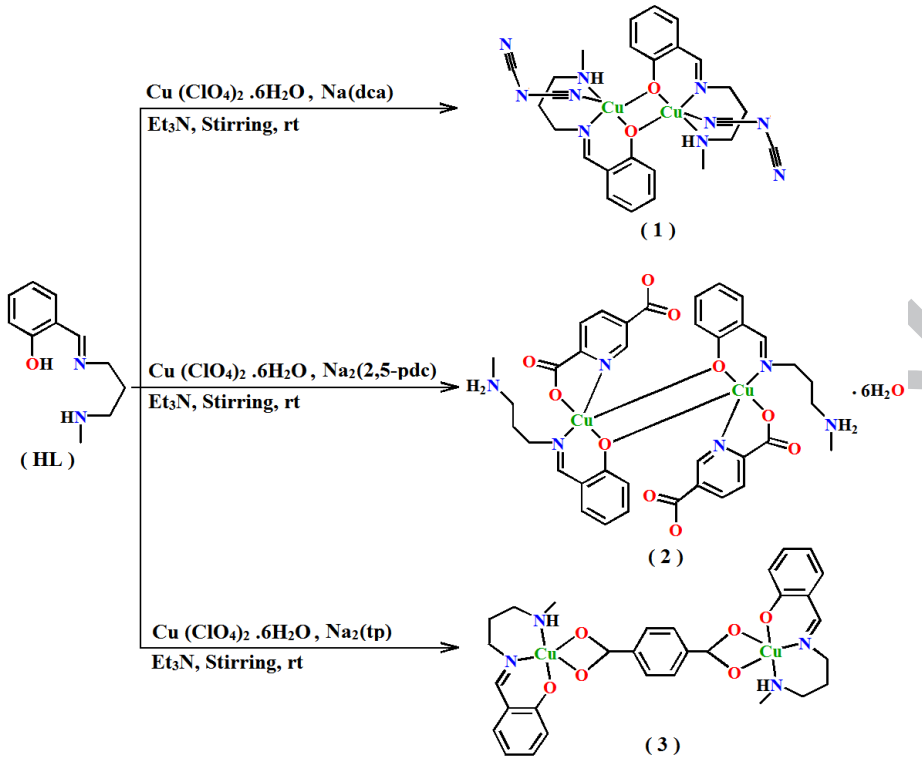

Scheme 1. Synthesis of **1**, **2** and **3**.

Synthesis of $[Cu_2L_2(dca)_2]$ ***(1)***.A methanolic solution (5 ml) of copper perchlorate hexahydrate (1 mmol, 0.370 g) was added to a mixture of HL (1 mmol, 0.192 g) and triethylamine (1 mmol, 0.10 g). To this resulting mixture an aqueous solution (5 ml) of sodium dicyanamide (1 mmol, 0.089 g) was added. The resulting deep green reaction mixture was stirred for 2 hours and filtered. Green single crystals suitable for X-ray diffraction quality were obtained after a few days on keeping the solution in a refrigerator. Yield 0.233g (73 %). $C_{26}H_{30}Cu_2N_{10}O_2$ (641.70): C, 48.66; H, 4.71; N, 21.82 %. Found: C, 48.65; H, 4.72; N, 21.82 (%). IR (cm^{-1}): 2975 (vs), 2944 (vs), 2885 (s), 2273 (s), 2219 (s), 2152 (s), 1643 (vs), 1554 (vs), 1466 (s), 1413 (vs), 1371 (s), 1298 (s), 1077 (s), 881 (s), 813 (s), 779 (s), 647 (s), 510 (s). MS (in MeOH, calcd m/z): 641.1170 ($C_{26}H_{30}Cu_2N_{10}O_2$).

Synthesis of $[Cu_2L_2(2,5\text{-}pdc)_2]\cdot 6H_2O$ ***(2)*** *and* $[Cu_2L_2(tp)]$ ***(3)***.The complexes **2** and **3** were synthesized by the same procedure as adopted for complex **1**, using disodium pyridine-2,5-

dicarboxylate (1 mmol, 0.211 g) and disodium terephthalate (0.5 mmol, 0.105g), respectively, instead of Sodium dicyanamide. For complex **2**; Yield 0.385g (81 %). $C_{36}H_{50}Cu_2N_6O_{16}$ (949.90): C, 45.52; H, 5.30; N, 8.80 %. Found: C, 45.51; H, 5.30; N, 8.81(%). IR (cm^{-1}): 3600-3200 (br, vs), 2980 (vs), 2944 (vs), 2885 (s), 1643 (vs), 1555 (vs), 1466 (s), 1414 (vs), 1372 (s), 1299 (s), 1078 (s), 882 (s), 815 (s), 783 (s), 639 (s). MS (in MeOH, calcd m/z): 841.1275 ($C_{36}H_{38}Cu_2N_6O_{10}$). For complex **3**; Yield 0.263g (78 %). $C_{30}H_{34}Cu_2N_4O_6$ (673.69): C, 53.48; H, 5.08; N, 8.31%. Found: C, 53.48; H, 5.07; N, 8.30 %. IR (cm^{-1}): 2977(vs), 2945(vs), 2893(s), 1643(vs), 1555(vs), 1466(s), 1413(vs), 1372(s), 1299(s), 1078(s), 882(s), 815(s), 783(s), 643(s). MS (in MeOH, calcd m/z): 674.1052 ($C_{30}H_{34}Cu_2N_4O_6$).

Crystallographic data collection and refinement

Data collection of complexes **1**, **2** and **3** were carried out by using a Nonius Kappa CCD diffractometer with graphite monochromated Mo-Kα radiation, at room temperature. The data sets were integrated with the Denzo-SMN package [10] and corrected for Lorentz, polarization and absorption effects (SORTAV) [11]. The structures were solved by direct methods using SIR97 [12] system of programs and refined using full-matrix least-squares with all non-hydrogen atoms anisotropically and hydrogens included on calculated positions, riding on their carrier atoms.All calculations were performed using SHELXL-97 [13] and PARST [14] implemented in WINGX [15] system of programs. Graphical programs used are those included in the WINGX System [15] and Diamond [16]. Crystal data and details of refinements are given in Table 1.

Cytotoxicity assay

Cell culture

MCF7 cells were grown in DMEM and MDA MB-231 cells were RPMI medium as monolayer supplemented with 10 % FBS, 100 U/ml penicillin and 100 µg/ml streptomycin at 37°C in a humid and 5% CO_2 atmosphere.

In vitro cytotoxicity assay

Cells were seeded at 5×10^3 cells per well in 96-well plates. Next day, cells were incubated with complexes **1** and **2**, with different concentrations (0 - 100 µM) for 48 hours and DMSO used as vehicle control. All the treatments were given in triplicate. MTT solution (20 µl of 5 mg/ml MTT) was added to each well following incubation with compounds for 48 hours and further incubated for 3.5 h at 37°C in a humid, 5% CO_2 atmosphere. Then, solution containing media was replaced by MTT solvent (iso-propanol, HCl and Triton X-100) and incubated for 15 min at room temperature with gentle rocking. The absorbance was read in Thermo Pierce Elisa plate reader at 570 nm. The results were expressed as percentage inhibition relative to the cells treated with DMSO (considered as 0 %). All the experiments were repeated for three times.

Immunoblotting assay

MDA-MB-231 cells were treated with the complex **1** (25 µM) and collected different time points (24 and 48 h) to check the apoptotic markers by immunoblotting. Cells were lysed and whole cell protein extracts were separated by SDS-PAGE and transferred onto PVDF membranes. After blocking with 3% nonfat dry milk in TBST for 1 h, the membranes were incubated with primary antibody against the indicated proteins for overnight at 4 °C. After washing with TBST, the membranes were incubated with horseradish peroxidase-conjugated secondary antibody for 1 h. Blots were developed using chemiluminescence methods in GE 4000 quantum chemiluminescence.

Cell cycle analysis

MDA-MB-231 cells were incubated with either with 25 µM complexes **1** or with 25 µM **2** for 48 h. Cells incubated with 0.1% DMSO were considered as control. At the end of the treatment, the cells were washed with ice cold PBS, fixed in 95% chilled ethanol and kept at 4°C for 24 h. On the day of FACS analysis, the fixed cells were again washed with ice cold PBS to remove the trace amount of ethanol and stained with the staining solution comprising 50 µg/ ml propidium iodide and 50 µg/ml RNAse in PBS. Cells were acquired on BD FACS Calibur instrument and the data was analysed using Cell Quest Pro software.

Albumin Binding studies

Electronic absorption spectral study

To maintain the physiological pH, solutions of bovine serum albumin (BSA)[17,18] (2.3 µM), human serum albumin (HSA)[18] (2.3 µM) and complexes (4 µM) solution were prepared in HEPES buffer. The interaction of complexes with serum albumins were studied by recording the change of electronic absorption spectra of BSA/HSA (2 ml 2.3 µM) with gradual addition of 10 µL 4 µM complexes at room temperature. The apparent association constant (K_{app}) [19] were calculated adopting the following equation

$$\frac{1}{(A_{obs} - A_0)} = \frac{1}{(A_c - A_0)} + \frac{1}{K_{app}(A_c - A_0)[complex]}$$

where, A_{obs} is the observed absorbance at 280 nm (characteristics band of BSA/HSA) at different concentration of complex. A_0 is the absorbance of serum albumin only.

Emission spectral study

BSA and HSA show characteristic emission bands at 341 nm (λ_{ex}, 280 nm) and 329 nm (λ_{ex}, 280 nm), respectively. The interaction of complexes with BSA (2.3 µM) and HSA (6.2 µM) were studied by gradual addition of 10 µL, 4 µM aqueous Cu(II) solution to 2 ml serum albumin solutions. The Stern-Volmer constants (K_{sv}) [20] and quenching rate constants (k_q) were calculated using the equations $F_0/F = 1 + K_{sv}$[complex] and $K_{sv} = k_q\tau_0$, where F_0 and F are the fluorescence intensity in the absence and in the presence of the complex, and τ_0 is the lifetime [21] of serum albumin (5×10^{-9} s). To calculate the binding constant of the complex with serum albumin, the following equation have been used $[(F_o–F)/F] = \log K_b + n \log$[complex], where K_b is the binding constant of the complex with serum albumin and n is the number of binding sites per albumin[22].

DNA binding experiments

Electronic absorption spectral study

Interaction of complexes **1-3** with CT-DNA were investigated using UV-vis absorption spectroscopic studies. For all the complexes, interaction have been studied by gradual addition of 10 µL, 15.6 µM solution of CT-DNA to 2 mL, 4 µM aqueous solution of complexes. Intrinsic binding constants (K_{ib}) [23] were determined using the following equation

$$\frac{[\mathrm{DNA}]}{(\varepsilon_a - \varepsilon_f)} = \frac{[\mathrm{DNA}]}{(\varepsilon_b - \varepsilon_f)} + \frac{1}{K_{ib}(\varepsilon_b - \varepsilon_f)}$$

where, [DNA] is the concentration of CT-DNA, ε_a is the extinction co-efficient value of the complex at a given CT-DNA concentration, ε_f and ε_b are the extinction co-efficient of the complex, in free solution and when fully bound to CT-DNA, respectively.

Competitive Ethidium bromide-DNA binding fluorescence measurement

When excited at 500 nm, ethidium bromide (EB) bounded CT-DNA shows emission band at 600 nm. Interaction of CT-DNA with complexes were studied flurometrically upon gradual addition of 10 µL 4 µM solution of complexes to the aqueous solution of EB bound CT-DNA (2 mL 8.5 µM) in HEPES buffer (pH 7.2). The Stern-Volmer constants (K_{sv}) were calculated using Stern-Volmer equation [20].

Molecular docking

Serum albumin - complex docking were performed by using AutoDock 4.2 software [24]. Crystal structure of BSA (PDB ID: 4f5s) and HSA (PDB ID: 1ao6), were downloaded from protein data bank (http://www.rcsb.org/pdb), and the Chimera program (http://www.cgl.ucsf.edu/chimera/) was used for receptor preparation. During docking calculation, the SAs were kept rigid and complexes being docked were kept flexible. The docking results were visualized by Chimera (http://www.cgl.ucsf.edu/chimera/) and PyMol software.

Results and discussion

Crystal structure description

Solid state structural analysis of **1-3** exhibit that all the compounds are dinuclear with five coordinated Cu(II) centre. Molecular structures of the complexes are shown in Figs.1-3. Bond length and bond angle are summarized in Table 2. In complex **1**, two [CuL(dca)] asymmetric units are connected through phenolic oxygens (O1a) and Cu(II) centres and form a base plane with phenyl ring (Fig. 1). Two dicyanamide (dca) units are placed in opposite direction and the dca units are perpendicular to the base plane. Largest bond length and bond angle of **1** are [Cu(1)-N(3), 2.087(4)Å] and [O(1a)-Cu(1)-N(1), 169.44(12)°], respectively and smallest

bond length and bond angle are [Cu(1)-N(1), 1.945(4)Å] and [O(1)-Cu(1)-O(1a), 79.53(12)°], respectively. In **2**, asymmetric unit of [CuL(2,5-pdc)] possesses planer structure and dimerises through phenolic oxygen (O1a) and Cu(II) centre with relatively larger copper oxygen bond length, 2.680Å (Fig. 2). Cu(1)-O(1a)[2.680(3)Å] and Cu(1)-O(1)[1.906(2)Å] are largest and smallest bond length, respectively. On the other hand O(1)-Cu(1)-O(2)[171.56(11)°] and O(1)-Cu(1)-O(1a) [79.70(9)] are largest and smallest bond angles, respectively. Crystal structure of **3** exhibits that Cu(L) units are connected through terephthalate ion(tp) (Fig. 3) and in this compound tp is perpendicular to copper(II)-Schiff base plane. Largest and smallest bond length in **3** are Cu(1)-O(3)[2.680(2)Å] and Cu(1)-O(1)[1.905(2)Å], respectively. O(2)-Cu(1)-N(1) [170.34(10)°] and O(2)-Cu(1)-O(3)[54.38(8)°] are largest and smallest bond angle, respectively.

Five coordinated complexes may possess either regular trigonal bipyramidal (TBP) or square pyramidal (SP) geometries. τ parameter [25] calculation allows to estimate deviations from TBP or SP ideal geometries. Regular TBP structure with D_{3h} symmetry has $\tau = 1$ and for a regular SP structure with C_{4v} geometry has $\tau = 0$. The τ values are calculated from the structural data and the values are 0.681, 0.060 and 0.163 for **1**, **2** and **3**, respectively (Table 2). The τ value indicate that **1** possesses TBP geometry, whereas **2** and **3** exhibit SP geometries, and in between **2** and **3**, complex **2** is more close to ideal SP geometry. It is interesting to note that most of the five coordinated copper(II) complexes possess SP geometry, however copper(II) centre in complex **1** possesses rare TBP coordination environment.

Packing structure of **1** exhibits that the dimeric units of **1** are connected through H-bonding [26] interactions (Table 1S) between the terminal dca nitrogen (N5) and imine hydrogen of Schiff base (N5···H26=2.212Å), forming a 1D supramolecular chain structure. These supramolecular 1D chains are connected through C-H...π interaction ($H\cdots C_g$= 3.232Å) (Table

2S), and form 2D supramolecular sheet like structure (Fig.1S). 2D supramolecular sheets are again interact with another type of C-H..π interaction [27] (H···C_g= 3.626Å),(Fig. 2S) which results 3D structure (Figs. 4 and 3S). Packing structure of **2** exhibits that the dimeric units are connected through H-bonding (Table 1S) between the free carboxylate of 2,5-pdc and imine hydrogen of Schiff base (O_4···H_{19}=2.180Å, O_5···H_{19}=2.115Å), forming 1D supramolecular chain (Fig. 4S). This 1D chains are again interacts through H-bonding with the lattice water molecules and form 2D supramolecular sheet like structure (Figs. 5 and 5S). It is interesting to note that the six lattice water molecules interact through H-bonding, and produced a twelve member cyclic supramolecular water cluster (Fig. 6S), where the oxygen atoms of six water molecules are arranged in a chair like conformation. Packing structure of **3** exhibits that the molecular units are connected through H-bonding interactions (O1···H2A = 2.018) (Table 1S) between phenolic oxygen and imine hydrogen of Schiff base, and form1D supramolecular chain structure. These 1D chains are again connected through C-H···π interaction (H···C_g= 2.755Å) (Table 2S), forming 2D supramolecular sheet like structure (Fig. 6). The 2D supramolecular sheets are again connected through another type of C-H..π interaction (H···C_g= 3.126Å) (Fig.7S) and build 3D supramolecular structure (Fig. 8S).

ESI mass spectrometry

ESI mass spectra of complexes were recorded using their methanolic solutions. Methanolic solutions of complexes were prepared 24 h before the mass spectral study. ESI-mass spectra of complexes show peaks at m/z = 641.1170 (for **1**), 841.1275 (for **2**) and 674.1052 (for **3**) corresponds to $[Cu_2L_2(dca)_2]^{\cdot+}$ (calc. = 641.70, for **1**), $[Cu_2L_2(2,5\text{-pdc})_2]^{\cdot+}$ (calc. = 841.81, for **2**) and $[Cu_2L_2(tp)]^{\cdot+}$(calc. = 673.69, for **3**) (Figs. 9S-11S). Mass spectral results indicate that complexes are stable in methanol and retain their dinuclear structure in solution.

Cytotoxic activity

The antiproliferative activity of **1** and **2** against human breast cancer cell line MCF7 and MDA-MB-231 has studied by standard 3-(4,5-dimethylthiazol-2-yl)-2,5-diphenyltetrazolium bromide (MTT) assay. Results demonstrated that **1** has better growth suppressor activity as compared to the **2** in both the cell lines. For example, the IC50 value of complexes **1** and **2** in MDA-MB0231 is 16.4 ± 1.6 and 43.2 ± 3.1 μM, respectively (Fig. 7). In addition, IC50 values of these compounds demonstrated that both compounds have more potent cytotoxic effect against triple negative breast cancer cell line MDA-MB-231 (more aggressive metastatic cell line) as compared to luminal A cell line MCF7 (less aggressive metastatic cell line). To understand whether the potent cytotoxic effect of these compounds is due to the induction of apoptosis, we performed cell cycle analysis. MDA-MB-231 cells were grown in the absence and presence of complex **1** for the indicated time periods and then analyzed the cell population by florescence activated cell sorting (FACS) analysis (Fig. 8a). Results revealed that population of cells at sub-G1 significantly increased with increasing periods of incubation complex **1** indicating that the complex might be promoting apoptosis through induction of DNA damage (Fig. 8a). To examine whether cytotoxic effect complex **1** is due to induction of apoptosis, immunoblotting was performed to examine the levels of pro-apoptotic and anti-apoptotic proteins following exposure of complex **1** for indicated time periods (Fig. 8b). Immunoblot results showed that expression levels of pro-apoptotic proteins are increased and in contrast expression levels of anti-apoptotic Bcl2 declined following exposure of complex **1** (Fig. 8b). Increased levels of p53, Bax and Apaf1 indicating that p53 might be playing important role in induction pro-apoptotic protein Bax at the transcriptional level. Increased Bax levels facilitate the polarization of mitochondrial membrane potential-mediated release cytochrome C. Released cytochrome C is then form complex with Apaf1 to promote the apoptosis induction. Results taken together suggest that complex **1** inhibits the

growth of cancer cells through induction of apoptosis-mediated cell death. A comparison of IC50 values of reported Cu(II) complexes are shown in Table 3.

Protein binding studies

Electronic absorption spectra of bovine serum albumin (BSA) and Human serum albumin (HSA) show the increase of absorbance with bathochromic shift (~20 nm) upon the gradual addition of complexes to serum albumin solutions (Figs. 9, 12S-16S). This bathochromic shift in electronic absorption spectra confirms ground state association of complexes with serum albumins. The calculated values of apparent association constants (K_{app}, L mol^{-1}) are 8.36 ± 1.62 × 10^5 (**1**-BSA), 16.90 ± 1.25 × 10^5 (**1**-HSA), 7.31 ± 1.05 × 10^5 (**2**-BSA), 11.00 ± 1.96 × 10^5 (**2**-HSA), 9.38 ± 1.34 × 10^5 (**3**-BSA), 17.19 ± 2.14 × 10^5 (**3**-HSA) (Table 4). The observed order of apparent association constant can be explain on the bases of the size of the molecules. Due to the small size, complex **1** is more interactive than **2**. On the other hand relatively high interaction affinity of **3** is due to its linear structure which favors the incorporation inside the protein moiety.

Fluorescence intensity of BSA and HSA considerably decreases (with slight blue shift) upon gradual increasing concentration of complexes (Figs. 9, 12S-16S). The Stern-Volmer constants (K_{sv}) and quenching rate constants (k_q) (Fig. 17S) indicate strong interaction between complex and serum albumin (Table 4). As electronic spectral change of serum albumins in presence of complexes indicate ground state association, and hence this fluorescence quenching is static in nature. Calculated values of binding constants (K_b, L mol^{-1}) are 2.42 ± 0.01 × 10^6 (**1**-BSA), 46.91 ± 0.02 × 10^6 (**1**-HSA), 2.33 ± 0.02 × 10^6 (**2**-BSA), 37.33 ± 0.02 × 10^6 (**2**-HSA), 7.22 ± 0.02 × 10^6 (**3**-BSA), 76.12 ± 0.03× 10^6 (**3**-HSA) (Table 3).

DNA binding studies of complexes

Aqueous solution of **1**-**3** show electronic absorption bands at 217 nm, 234 nm, 266 nm and 354 nm for **1**; 216 nm, 264 nm, 270 nm and 343 nm for **2**; 218 nm, 235 nm, 264 nm and 354 nm for **3**. On gradual addition of CT-DNA, for **1**, electronic absorbance of 266 nm band gradually increases with blue shift and finally the band appears at 259 nm, whereas absorbance of 354 nm band gradually decreases. An isobestic point in the titration curve (Fig. 10) at 336 nm indicates the presence of more than two species in the medium [30]. Upon gradual addition of CT-DNA to the solutions of **2** and **3** the absorbance at 264 nm band gradually increases with blue shift and finally the band appear at 258 nm and 254 nm, respectively (Figs. 18S and 19S). Calculated values of intrinsic binding constants (K_{ib}) are $1.52 \pm 0.08 \times 10^5$, $2.50 \pm 0.12 \times 10^5$ and $10.07 \pm 0.56 \times 10^5$ L mol^{-1} for complexes **1**, **2** and **3**, respectively (Table 5). K_{ib} of the complexes are determined with respect to the wavelength 259 nm, 258 nm and 254 nm for **1**, **2** and **3,** respectively.

Fluorescence intensity of ethidium bromide (EtBr) increases strongly in presence of CT-DNA due to its strong intercalation with CT-DNA [32]. On excitation at 500 nm, CT-DNA bounded EtBr shows emission at 608 nm. A quenching of fluorescence intensity is observed when complex solutions were added to the aqueous solutions of EtBr-CT-DNA (Fig. 20S-22S). This is due to the interaction of complexes with DNA, where complex molecule displaces the ethidium bromide molecules from the interactive side of DNA. From the Stern-Volmer equation linear relationships (Fig. 23S) were obtained from the titration of CT-DNA bounded EtBr, using complexes as quencher. The calculated values of binding constants (K_{sv}) are $13.63 \pm 0.01 \times 10^6$, $13.80 \pm 0.02 \times 10^6$ and $16.69 \pm 0.02 \times 10^6$ L mol^{-1} for **1**, **2** and **3**, respectively (Table 5).**Protein-complex docking**

Molecular docking studies have been carried out to understand the nature of binding nature in between complexes and serum albumins. Chimera scores of the individual complexes with different poses have been tabulated in Table 3S. Since BSA and HSA have two different

active sites (*Tyr 149* and *Tyr 410* for BSA; *Tyr 150* and *Tyr 411* for HSA) for binding, we performed docking of each complex with two binding sites individually in order to investigate effective binding site of BSA and HSA for our complexes. Based on the chimera score it is clear that complexes **1-3** selectively bind with BSA at the site of *Tyr 149*, and that of HSA at the site of *Tyr 150*. Moreover, chimera score also indicate that complex **3** binds more effectively with serum albumins in comparison to **1** and **2**. Binding interaction of the complexes with the RCSB protein are shown in Figs. 11, 24S-34S.The dock results indicate that complexes **1-3** form hydrogen bonding with HSA when interact with its *Tyr150* site. But only **2** forms hydrogen bond with HSA when interacts at *Tyr411* site of HSA (Table 6).

In addition to hydrogen bonding interaction, we also analyzed the hydrophobic and van der Waals interaction of complexes with serum albumins and the results are tabulated in Table 4S. The analysis indicate that hydrophobic amino acids of SA that are interacting with complexes are: for complex **1**, Leu237 (active site *Tyr149*) and Leu386 (active site *Tyr410*) of BSA; for complex **2**, Phe148, Ala290 (active site *Tyr149*) and Leu386, Leu406, Leu429, Leu452 (active site *Tyr410*) of BSA and Val241, Ala291 (active site *Tyr150*) and Ala194, Val455 (active site *Tyr411*) of HSA; for complex **3**,Phe148, Val186, Leu237, Ala290 (active site *Tyr149*) and Leu386, Leu406, Leu429, Leu452 (active site *Tyr410*) of BSA and Ala191, Leu238 (active site *Tyr150*) and Ala194, Val455 (active site *Tyr411*) of HSA. The polar amino acids that are interacting with complexes are: for **1**,Tyr149, Glu152, Tyr156, Trp213, His241 (active site *Tyr149*) and Asn390, Tyr410 (active site *Tyr410*) of BSA and Cys448, Tyr452 (active site *Tyr411*) of HSA; for **2**,Tyr149, Glu152, Tyr156, Trp213, His241 (active site *Tyr149*) and Asn390, Tyr410, Ser488 (active site *Tyr410*) of BSA and Gln196 (active site *Tyr150*) and Trp214, Tyr452 (active site *Tyr411*) of HSA; for **3**,Tyr149, Glu152, Tyr156, Ser191, Ser192, Gln195, His241, His287 (active site *Tyr149*) and Asn390, Tyr410, Thr448,

Ser488 (active site *Tyr410*) of BSA and Tyr150, Ser192, Trp214, His242 (active site *Tyr150*) and Gln459, Tyr452 (active site *Tyr411*) of HSA.

Conclusion

We have presented here synthesis, crystal structure and biological activities of three dinuclear 2-[(3-Methylamino-propylimino)-methyl]-phenol (HL) coordinated copper(II) complexes using N/O donor anionic ligands. Copper(II)-L in combination with anionic ligands dca (**1**), 2,5-pdc (**2**) and tp (**3**) generates discrete dinuclear complexes. In **1** and **3**, HL shows a tridentate (N,N,O) chelating coordination mode, whereas in **2**, it functions as bidentate (N,O) chelating ligand. Copper(II) centres in complexes **2** and **3** possess square pyramidal (SP) geometry whereas in complex **1** copper(II) centres possess rare trigonal bipyramidal (TBP) geometry. 3D supramolecular architecture in **1** and **3** are formed with H-bonding and C-H…π interactions, whereas only H-bonding interactions results 2D supramolecular structure in **2**. Anticancer activities of **1** and **2** in human breast cancer cell lines MCF7 and MDA-MB-231 show that **1** has better growth suppressor activity in comparison to **2** through induction of apoptosis. Study of the kinetics of interactions of **1-3** with CT-DNA and serum albumins show that the complexes effectively binds with CT-DNA and serum albumins and the order of interaction is **3**>**1**>**2**. This order of interaction has been explained on the basis of size and shapes of the compounds. Molecular docking study indicates that complexes **1** and **3** interact with *Tyr150* site of human serum albumin, whereas complex **2** interacts with *Tyr150 and Tyr411* sites of human serum albumin through hydrogen bonding interaction. In addition to H-bonding, hydrophobic and van der Waals interactions are also responsible for albumin and complex interactions.

Acknowledgements

This work was supported by the UGC Innovative Research Program (VU / Innovative / Sc / 08 / 2015) of Vidyasagar University, India. Dr. S. C. Manna thanks UGC-SAP and DST-FIST New Delhi and Vidyasagar University for infrastructural facilities. Authors are also thankful to Prof. V. Bertolasi (Universita di Ferrara) for structural data collection of complex **3**.

Supplementary information

CCDC 1813748-1813750contain the supplementary crystallographic data for this article. These data can be obtained free of charge viahttp://www.ccdc.cam.ac.uk/conts/retrieving.html, or from the Cambridge Crystallographic Data Centre, 12 Union Road, Cambridge CB2 1EZ, UK; fax: (+44) 1223-336-033; or e-mail: deposit@ccdc.cam.ac.uk. Results of spectroscopic studies (electronic absorption spectra, emission spectra, IR spectra, NMR, ESI mass), Figures of crystal structures and biological studies are provided as supplementary material.

References

[1] (a) Z. Zhang, H. Zhao, M.M. Matsushita, K. Awaga, K.R. Dunbar, J. Mater. Chem. C 2 (2014) 399-404; (b) I.-H. Park, A. Chanthapally, Z. Zhang, S.S. Lee, M.J. Zaworotko, J.J. Vittal, Angew. Chem., Int. Ed. 53 (2014) 414-419; (c) S.R. Batten, R. Robson, Angew. Chem., Int. Ed. 37 (1998) 1460-1494.

[2] (a) C. Santini,M. Pellei,V. Gandin,M. Porchia, F. Tisato, C. Marzano, Chem. Rev. 114 (2014) 815-862; (b) B. Duff, V.R. Thangella, B.S. Creaven, M. Walsh, D.A. Egan, Eur. J. Pharma. 689 (2012) 45-55; (c) A.T. Chaviara, P.C. Christidis, A. Papageorgiou, E. Chrysogelou, D.J. Hadjipavlou-Litina, C.A. Bolos, J. Inorg. Biochem. 99 (2005) 2102-2109;

(d) S.K. Tripathy, R.K. Surada, R.K. Manne, S.M. Mobin, M.K. Santra, S. Patra, Dalton Trans. 42 (2013) 14081-14091.

[3] (a) F. Mancin, P. Scrimin, P. Tecilla, U. Tonellato, Chem. Commun. (2005) 2540-2548; (b) M. Pitié, C.J. Burrows, B. Meunier, Nucleic Acids Res. 28 (2000) 4856-4864; (c) B. Maity, M. Roy, S. Saha, A.R. Chakravarty, Organometallics 28 (2009) 1495-1505; (d) J.A. Cowan, A. Sreedhara, J. Biol. Inorg. Chem. 6 (2001) 337-347; (e) M.E. Branum, A.K. Tipton, S. Zhu, Jr. L. Que, J. Am. Chem. Soc. 123 (2001) 1898-1904.

[4] P. Kumar, S. Gorai, M.K. Santra, B. Mondal, D. Manna, Dalton Trans. 41 (2012) 7573-7581.

[5] (a) A. Tarushi, J. Kljun, I. Turel, A.A. Pantazaki, G. Psomas, D.P. Kessissoglou, New J. Chem. 37 (2013) 342-355; (b) W.H. Ang, E. Daldini, L. Juillerat-Jeanneret, P.J. Dyson, Inorg. Chem. 46 (2007) 9048-9050; (c) T. Kosta, T. Maryama, M. Otagiri, Pharm. Res. 14 (1997) 1607-1612.

[6] R. Loganathan,S. Ramakrishnan,E. Suresh,A. Riyasdeen, M.A. Akbarsha, M. Palaniandavar, Inorg. Chem, 51 (2012) 5512-5532.

[7] S. Naiya, S. Biswas, M.G.B. Drew, C.J. Gómez-García, A. Ghosh, Inorg. Chim. Acta 377 (2011) 26-33.

[8] D.D. Perrin, W.L.F. Armarego, D.R. Perrin, Purification of Laboratory Chemicals; Pergamon Press: Oxford, U.K. (1980).

[9] J.R. Lakowicz, Principles of Fluorescence Spectroscopy, Third Edition, Springer, New York, USA (2006).

[10] Z. Otwinowski, W. Minor, Methods in Enzymology, C.W. Carter, R.M. Sweet Editors, Part A, Academic Press, London 276 (1997) 307-326.

[11] R.H. Blessing, Acta Crystallogr. Sect A 51 (1995) 33-38.

[12] A. Altomare, M.C. Burla, M. Camalli, G.L. Cascarano, C. Giacovazzo, A. Guagliardi, A.G. Moliterni, G. Polidori, R. Spagna, J. Appl. Crystallogr. 32 (1999) 115-118.

[13] G.M. Sheldrick, SHELX-97, Program for Crystal Structure Refinement, University of Gottingen, Germany (1997).

[14] M. Nardelli, J. Appl. Crystallogr. 28 (1995) 659.

[15] L. Farrugia, J. Appl. Crystallogr. 32 (1999) 837-838.

[16] K. Brandenburg, DIAMOND (Version 3.2i), Crystal Impact GbR, Bonn, Germany (1999).

[17] X.-Q. Zhou, Q. Sun, L. Jiang, S.-T. Li, W. Gu, J.-L. Tian, X. Liu, S.-P. Yan, Dalton Trans. 44 (2015) 9516-9527.

[18] A. Tarushi, E. Polatoglou, J. Kljun, I. Turel, G. Psomas, D.P. Kessissoglou, Dalton Trans. 40 (2011) 9461-9473.

[19] (a) S. Mistri , H. Puschmann , S.C. Manna, Polyhedron 115 (2016) 155-163 (b) F. Samari, B. Hemmateenejad, M. Shamsipur, M. Rashidi, H. Samouei, Inorg. Chem. 51 (2012) 3454-3464.

[20] S. Veeralakshmi, S. Nehru, S. Arunachalam, P. Kumar, M. Govindaraju, Inorg. Chem. Front. 1 (2014) 393-404.

[21] F.-F. Tian, J.-H. Li, F.-L. Jiang, X.-L. Han, C. Xiang, Y.-S. Ge, L.-L. Li, Y. Liu, RSC Advances 1 (2012) 501-513.

[22] H.F. Crouse, J. Potoma, F. Nejrabi, D.L. Snyder, B.S. Chohanb, S. Basu, Dalton Trans. 41 (2012) 2720–2731.

[23] (a) L. Subha, C. Balakrishnan, S. Thalamuthu, M.A. Neelakantan, J. Coord. Chem. 68 (2015) 1021-1039.

[24] Y.-X. Si, Z.-J. Wang, D. Park, H.Y. Chung, S.-F. Wang, L. Yan, J.-M. Yang, G.-Y. Qian, S.-J. Yin, Y.-D. Park, Int. J. Bio.Macro. 50 (2012) 257-262.

[25] A.W. Addison, T.N. Rao, J. Reedijk, J.V. Rijn, G.C. Verschoor, J. Chem. Soc. Dalton Trans. (1984) 1349-1356.

[26] M.C. Etter, J.C. MacDonald Bernstein, J. Acta Crystallogr. B46 (1990) 256-262.

[27] M. Nishio, M. Hirota, Y. Umezawa, The C−H···π Interaction: Evidence, Nature and Consequences, Wiley-VCH, New York (1998).

[28] (a) P. Nagababu, A.K. Barui, B. Thulasiram, C.S. Devi, S. Satyanarayana, C.R. Patra, B. Sreedhar, J. Med. Chem. 58 (2015) 5226-5241; (b) R. Dhivya, P. Jaividhya, A. Riyasdeen, M. Palaniandavar, G. Mathan, M.A. Akbarsha, Biometals 28 (2015) 929-943; (c) A. Bhunia, S. Manna, S. Mistri, A. Paul, R.K. Manne, M.K. Santra, V. Bertolasic, S.C. Manna, RSC Adv. 5 (2015) 67727-67737; (d) S. Mistri, A. Paul, A. Bhunia, R.K. Manne, M.K. Santra, H. Puschmann, S.C. Manna, Polyhedron 104 (2016) 63-72.

[29] (a) A. Paul, A. Figuerola, V. Bertolasi, S.C. Manna, Polyhedron 119 (2016) 460-470; (b) N. Biswas, S. Khanra, A. Sarkar, S. Bhattacharjee, D.P. Mandal, A. Chaudhuri, S. Chakraborty, C.R. Choudhury, New J. Chem. 41 (2017) 12996-13011; (c) S. Dolai, K. Das, A. Bhunia, V. Bertolasi, S.C. Manna, Appl. Organomet. Chem. 2018, 32:e4506.

[30] P.O. Vardevanyan, V.L. Élbakyan, M.A. Shahinyan, M.V. Minasyants, M.A. Parsadanyan, N.S. Sahakyan, J. Appl. Spectrosc. 81 (2015) 1060-1063.

[31] (a) A. Paul, S. Mistri, A. Bhunia, S. Manna, H. Puschmann, S.C. Manna, RSC Adv. 6 (2016) 60487- 60501; (b) T.S. Mahapatra, A. Roy, S. Chaudhury, S. Dasgupta, S.L. Shrivastava, V. Bertolasi, D. Ray, Eur. J. Inorg. Chem. (2017) 769-779; (c) F. Arjmand, Z. Afsan, T. Roisnelb, RSC Adv. 8 (2018) 37375-37390.

[32] (a) Q.-L. Zhang, J.-G. Liu, H. Chao, G.-Q. Xue, L.-N. Ji, J. Inorg. Biochem. 83 (2001) 49-55; (b) Z.-C. Liu, B.-D. Wang, B. Li, Q. Wang, Z.-Y. Yang, T.-R. Li, Y. Li, Eur. J. Med. Chem. 45 (2010) 5353-5361; (c) F. Mancin, P. Scrimin, P. Tecilla, U. Tonellato, Chem.

Commun. (2005) 2540-2548; (d) L. Tjioe, A. Meininger, T. Joshi, L. Spiccia, B. Graham, Inorg. Chem. 50 (2011) 4327-4339.

Table 1. Crystal data and structure refinement for complexes **1**-**3**.

Complex	**1**	**2**	**3**
Empirical formula	$C_{26}H_{30}Cu_2N_{10}O_2$	$C_{36}H_{50}Cu_2N_6O_{16}$	$C_{30}H_{34}Cu_2N_4O_6$
Formula mass, g mol^{-1}	641.70	949.90	673.69
Crystal system	Triclinic	Triclinic	Monoclinic
Space group	P-1	P-1	P21/c
a, Å	8.883(5)	7.9884(16)	9.5456(9)
b, Å	9.080(5)	11.211(2)	10.7836(13)
c, Å	10.432(5)	12.760(3)	14.0349(16)
α, deg	97.961(5)	69.66(3)	90
β, deg	112.838(5)	84.98(3)	99.524(8)
γ, deg	111.247(5)	80.76(3)	90
Z	1	1	2
V, Å^3	683.5(6)	1057.0(4)	1424.8(3)
$D_{(calcd)}$, g cm^{-3}	1.559	1.492	1.570
μ(Mo-Ka), mm^{-1}	1.600	1.083	1.544
F(000)	330	494	696
θ_{min}-θ_{max}, deg	4.3-25	4.1-25	3.4-27.5
No. of collected data	4606	14835	8749
No. of unique data	2394	3711	3052
R_{int}	0.029	0.160	0.032
Observed reflections [$I > 2\sigma(I)$]	2193	2520	2479
Goodness of fit (F^2)	1.087	0.852	1.041
Parameters refined	186	281	191
*R*1, *wR*2 (all data) [a]	0.0418, 0.1135	0.0563, 0.1492	0.0431, 0.1150
Residuals, e Å^{-3}	-0.54, 1.60	-0.65, 0.71	-0.41, 0.55

[a] $R1(Fo) = \Sigma \big| |Fo| - |Fc| \big| / \Sigma |Fo|$, $wR2(Fo^2) = [\Sigma w (Fo^2 - Fc^2)^2 / \Sigma w (Fo^2)^2]^{½}$

Table 2. Experimental coordination bond lengths (Å) and angles (°) for complexes **1**-**3**.

1		**2**		**3**	
Cu(1)-O(1)	2.041(3)	Cu(1)-O(1)	1.906(2)	Cu(1)-O(1)	1.905(2)
Cu(1)-N(1)	1.945(4)	Cu(1)-O(2)	1.963(2)	Cu(1)-O(2)	1.990(2)
Cu(1)-N(2)	2.030(4)	Cu(1)-N(1)	1.958(4)	Cu(1)-O(3)	2.680(2)
Cu(1)-N(3)	2.087(4)	Cu(1)-N(2)	2.017(4)	Cu(1)-N(1)	1.955(3)
Cu(1)-O(1a)	1.965(3)	Cu(1)-O(1a)	2.680(3)	Cu(1)-N(2)	2.009(3)
O(1)-Cu(1)-N(1)	90.56(12)	O(1)-Cu(1)-O(2)	171.56(11)	O(1)-Cu(1)-O(2)	85.36(9)
O(1)-Cu(1)-N(2)	128.54(13)	O(1)-Cu(1)-N(1)	94.73(13)	O(1)-Cu(1)-O(3)	87.17(9)
O(1)-Cu(1)-N(3)	105.38(13)	O(1)-Cu(1)-N(2)	91.27(13)	O(1)-Cu(1)-N(1)	93.54(10)
O(1)-Cu(1)-O(1a)	79.53(12)	O(1)-Cu(1)-O(1a)	79.70(9)	O(1)-Cu(1)-N(2)	160.52(10)
N(1)-Cu(1)-N(2)	89.74(14)	O(2)-Cu(1)-N(1)	93.48(13)	O(2)-Cu(1)-O(3)	54.38(8)
N(1)-Cu(1)-N(3)	93.48(14)	O(2)-Cu(1)-N(2)	81.03(13)	O(2)-Cu(1)-N(1)	170.34(10)
O(1a)-Cu(1)-N(1)	169.44(12)	O(1a)-Cu(1)-O(2)	96.74(9)	O(2)-Cu(1)-N(2)	88.28(10)
N(2)-Cu(1)-N(3)	125.97(15)	N(1)-Cu(1)-N(2)	167.94(15)	O(3)-Cu(1)-N(1)	116.01(10)
O(1a)-Cu(1)-N(2)	93.57(14)	O(1a)-Cu(1)-N(1)	101.33(12)	O(3)-Cu(1)-N(2)	103.98(9)
O(1a)-Cu(1)-N(3)	92.70(14)	O(1a)-Cu(1)-N(2)	90.03(11)	N(1)-Cu(1)-N(2)	95.71(11)
Cu(1)-O(1)-Cu(1a)	100.47(13)	Cu(1)-O(1)-Cu(1a)	100.30(10)		
τ_5 parameter	0.681		0.060		0.163

Table 3. IC_{50} values of Cu(II) complexes at μM level.

Complex	IC50		Ref
	MCF7	MDA-MB-231	
1	26±2.9	16.4±1.6	This work
2	51±4.7	43.2±3.1	This work
$[Cu(Tf\text{-}PIP)_2(H_2O)]^{2+}$		0.6 ± 0.03	[28a]
$[Cu(PYIP)_2(H_2O)]^{2+}$		26.5 ± 1.5	[28a]
$[Cu(CN\text{-}PIP)_2(H_2O)]^{2+}$		40.0 ± 4.6	[28a]
$[Cu(PIP)_2(H_2O)]^{2+}$		0.1 ± 0.005	[28a]
$[Cu(L^1)(diimine)]^{+}$	0.59 ± 0.01	0.96 ± 0.02	[28b]
$[Cu(L^2)(H_2O)]\cdot ClO_4$	31.07±6.67		[28c]
$[Cu(L^3)(H_2O)]\cdot ClO_4$	42.63±7.13		[28c]
$[Cu(L^4)(H_2O)]\cdot ClO_4$	>100		[28c]
$\{[Cu(HL^5)(pdc)(H_2O)]\cdot [Cu(HL^5)(pdc)]\cdot 10.5(H_2O)\}$	47 ± 5.2		[28d]

IP= Imidazophenanthroline ligands, HL^1 = 2-[(2-dimethylaminoethylimino)methyl]phenol, diimine = dipyrido[3,2-a:20,30-c]phenazine (dppz), HL^2 = o-{[2-(2-aminoethylamino)ethylimino]methyl}phenol; HL^3 = 2-{[2-(2-aminoethylamino) ethylimino]methyl}-6-methoxyphenol; HL^4 = o-{1-[2-(2-aminoethylamino)ethylimino]ethyl}phenol, HL^5= 6-methoxy-2-{[2-(1-piperazinyl)ethylimino]methyl}phenol, pdc = pyridine 2,5-dicarboxylate.

Table 4. Kinetic parameters of BSA / HSA interaction of Cu(II) complexes.

Complex-albumin	K_{app} ($L\ mol^{-1}$)	K_{sv} ($L\ mol^{-1}$)	K_b ($L\ mol^{-1}$)	k_q ($L\ mol^{-1}\ s^{-1}$)	n	Ref
1-BSA	$8.36 \pm 1.62 \times 10^5$	$11.60 \pm 0.03 \times 10^6$	$2.42 \pm 0.01 \times 10^6$	23.20×10^{14}	0.96	This work
1-HSA	$16.90 \pm 1.25 \times 10^5$	$16.40 \pm 0.08 \times 10^6$	$46.91 \pm 0.02 \times 10^6$	32.80×10^{14}	1.09	This work
2-BSA	$7.31 \pm 1.05 \times 10^5$	$9.87 \pm 0.01 \times 10^6$	$2.33 \pm 0.02 \times 10^6$	19.75×10^{14}	0.94	This work
2-HSA	$11.00 \pm 1.96 \times 10^5$	$16.00 \pm 0.06 \times 10^6$	$37.33 \pm 0.02 \times 10^6$	32.00×10^{14}	1.09	This work
3-BSA	$9.38 \pm 1.34 \times 10^5$	$12.07 \pm 0.07 \times 10^6$	$7.22 \pm 0.02 \times 10^6$	24.15×10^{14}	1.01	This work
3-HSA	$17.19 \pm 2.14 \times 10^5$	$17.14 \pm 0.10 \times 10^6$	$76.12 \pm 0.03 \times 10^6$	34.28×10^{14}	1.13	This work
$\{[Cu_2(L^1)_2(fum)]\cdot(H_2O)\cdot(MeOH)\}n$-BSA	1.34×10^4	2.09×10^5	7.83×10^5	4.1866×10^{13}	1.34	[29a]
$\{[Cu_2(L^1)_2(fum)]\cdot(H_2O)\cdot(MeOH)\}n$-HSA	1.81×10^4	1.39×10^5	7.55×10^5	2.794×10^{13}	1.14	[29a]

$[Cu_2(L^2)_2(N_3)_2]$-BSA		8.24×10^4	2.92×10^5	5.15×10^{12}	1.06	[29b]
$[Cu2(L^2)_2(N_3)_2]$-HSA		7.57×10^4	1.28×10^5	4.73×10^{12}	1.39	[29b]
$[Cu_2(L^3)_2(mb)]\cdot ClO_4$-BSA	1.7×10^5	4.4×10^5	4.7×10^5	4.4×10^{13}	0.70	[29c]
$[Cu_2(L^3)_2(mb)]\cdot ClO_4$-HSA	1.6×10^5	4.8×10^5	4.9×10^5	4.8×10^{13}	0.70	[29c]
$[Cu_2(L^4)_2(mb)]\cdot ClO_4$-BSA	5.7×10^5	5.2×10^5	5.8×10^5	5.2×10^{13}	0.76	[29c]
$[Cu_2(L^4)_2(mb)]\cdot ClO_4$-HSA	6.9×10^5	4.9×10^5	5.7×10^5	4.9×10^{13}	1.02	[29c]

HL^1 derived from the condensation reaction of 2-amino-1-butanol and salicylaldehyde; fum^{2-}= fumarate; HL^2 derived from the condensation reaction of 2-acetylpyridine and thiosemicarbazide; HL^3 = 2-[(2-diethylaminoethylimino)methyl]phenol; HL^4 = 2-[1-(2-diethylaminoethylimino)propyl]phenol; mb = 4-methylbenzoate

Table 5. Kinetic parameters of CT-DNA interaction of Cu(II) complexes.

Complex	K_b	K_{sv} (L mol^{-1})	Ref
1	$1.52 \pm 0.08 \times 10^5$	$13.63 \pm 0.01 \times 10^6$	This work
2	$2.50 \pm 0.12 \times 10^5$	$13.80 \pm 0.02 \times 10^6$	This work
3	$10.07 \pm 0.56 \times 10^5$	$16.69 \pm 0.02 \times 10^6$	This work
$[Cu(L^1)(pa)]$	1.68×10^5	14.05×10^4	[31a]
$[Cu(L^1)(mb)]$	2.27×10^5	19.90×10^4	[31a]
$\{[Cu_2(L^2)_2(fum)](H_2O)(MeOH)\}n$	2.96×10^5	1.71×10^5	[29a]
$[Cu_4(\mu\text{-}L^3)_2(\mu_{1,1,3,3}\text{-}O_2CH)](OH)_6H_2O$	3.37×10^4	4.73×10^4	[31b]
$[Cu(L^4)(phen)(NO_3)]$	5.81×10^4	6.12×10^4	[31c]
$[Cu(L^4)(bpy)(NO_3)]$	2.50×10^4	3.80×10^4	[31c]

$[Cu(L^4)(DACH)(NO_3)]$	3.05×10^4	4.68×10^4	[31c]
$[Cu(bba)(bpy))]^{2+}$	$(0.06 \pm 0.07) \times 10^5$	1.7×10^5	[6]
$[Cu(bba)(phen)]^{2+}$	$(0.28 \pm 0.04) \times 10^5$	3.6×10^5	[6]
$[Cu(bba)(5,6\text{-dmp})]^{2+}$	$(1.09 \pm 0.39) \times 10^5$	1.08×10^6	[6]
$[Cu(bba)(dpq)]^{2+}$	$(2.20 \pm 0.34) \times 10^5$	5.1×10^5	[6]

HL^1= o-{(3-morpholinopropylimino)methyl}phenol, pa= 3-phenylacrylate, mb= p-methylbenzoate, fum= fumarate, Schiff base (HL^2) derived from the condensation reaction of 2-amino-1-butanol and salicylaldehyde. H_3L^3 = 1,3-bis [3-aza-3-(1-methyl-3-oxobut-1-enyl)prop-3-en-1-yl]-2-(2-hydroxyphenyl)-1,3-imidazolidine, L^4= 3-formylchromone, phen= 1,10-phenanthroline, bpy= 2,2′ -bipyridine, DACH= 1R,2R-DACH, bba= N,N-bis(benzimidazol-2-ylmethyl)-amine, 5,6-dmp= 5,6-dimethyl-1,10-phenanthroline, dpq= dipyrido[3,2-d:2,3-f] quinoxaline.

Table 6.Hydrogen bonding interactions for complexes **1-3** with HSA.

Complex	H bonds	D···A (Å)	D-H···A (Å)
1 (Active site: Tyr150)	N-H (His816)···N	2.436	1.641
2 (Active site: Tyr150)	N-H (Lys773)···O	3.307	2.547
2 (Active site: Tyr411)	N-H (Lys436)···O	2.739	1.956
3 (Active site: Tyr150)	N-H (Gln196)···O	3.016	2.100

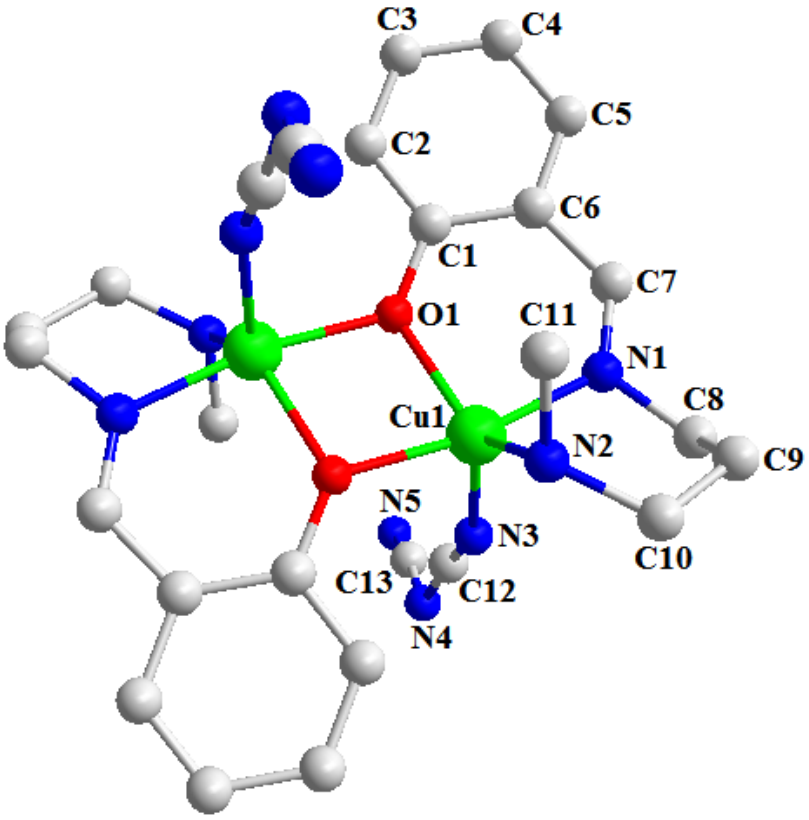

Fig. 1. Molecular structure of complex **1**.

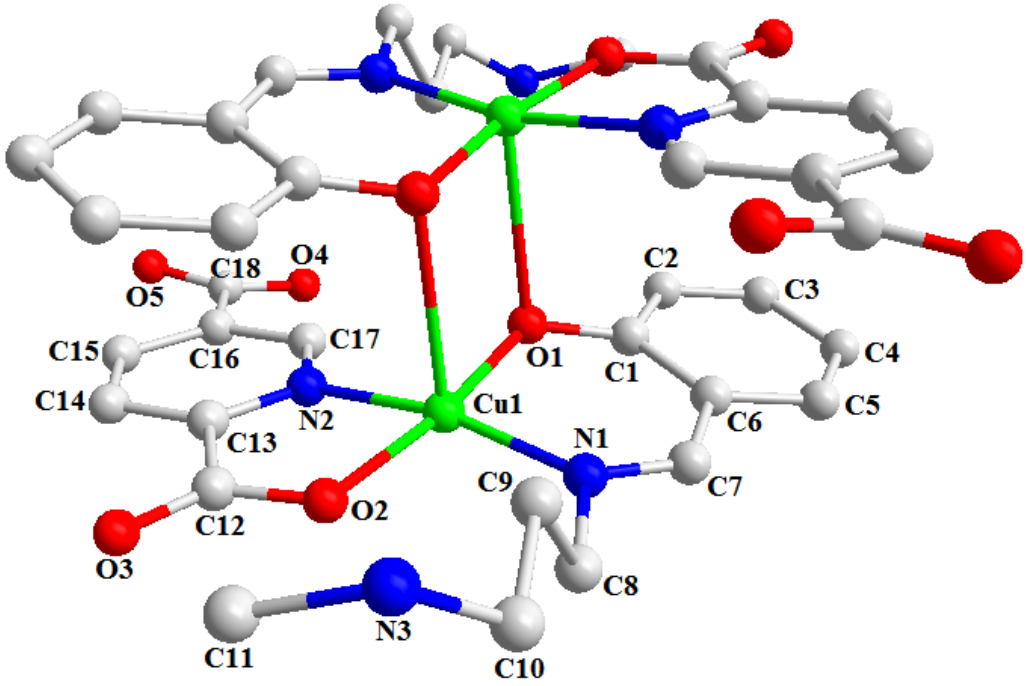

Fig. 2. Molecular structure of complex **2** (water molecules are omitted for structural clarity).

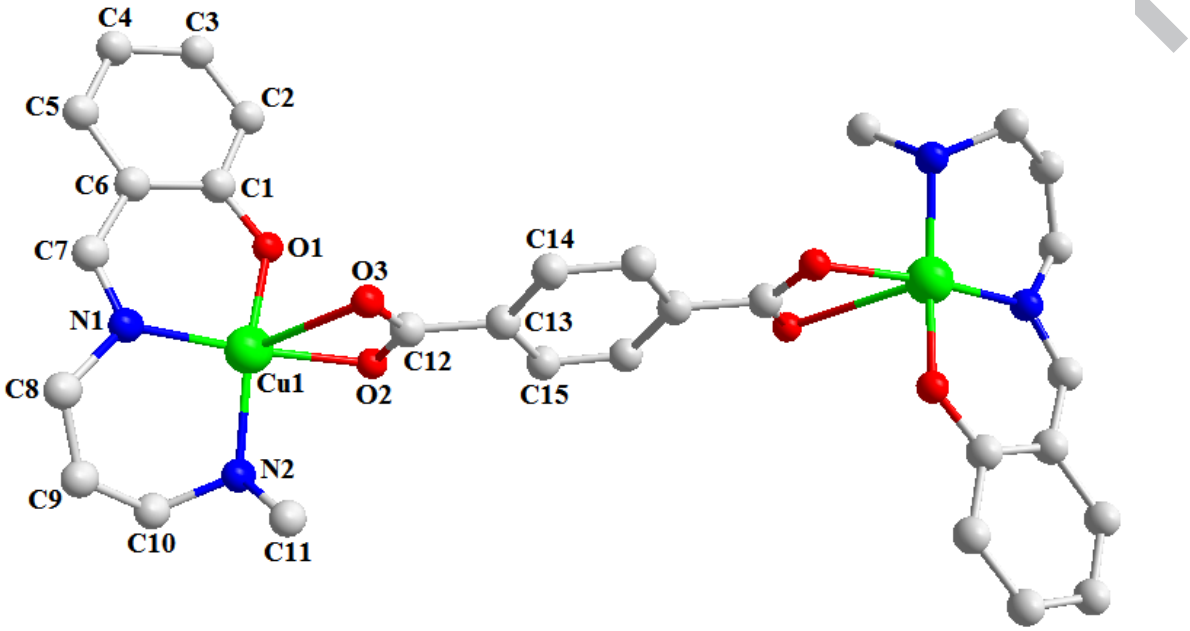

Fig. 3. Molecular structure of complex **3**.

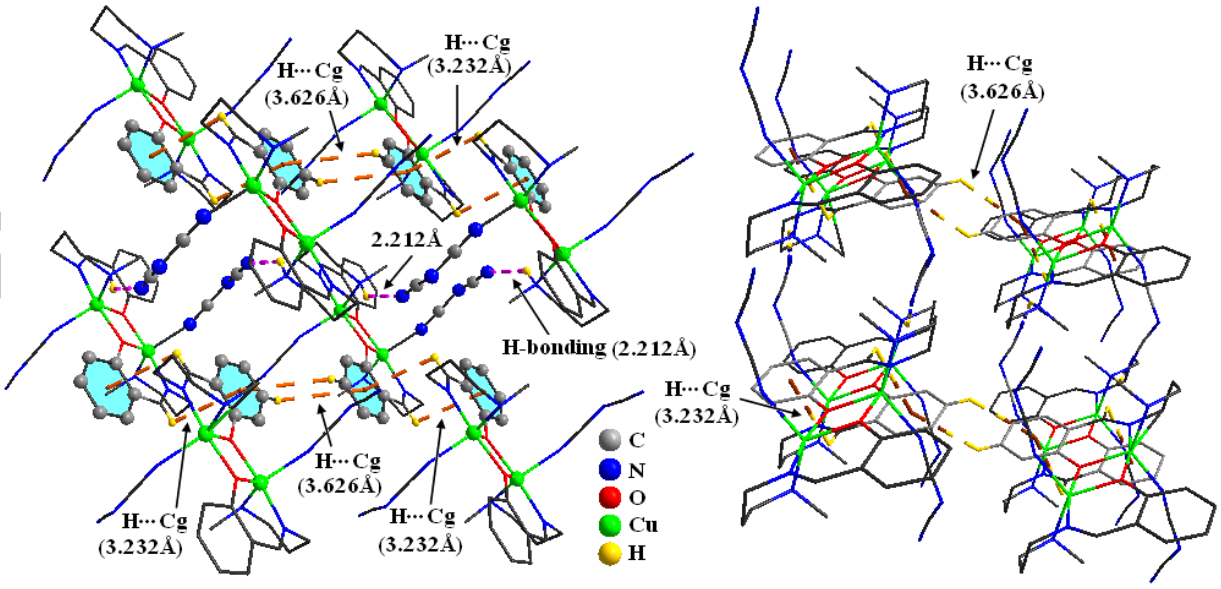

Fig. 4. 3D supramolecular structure of **1**.

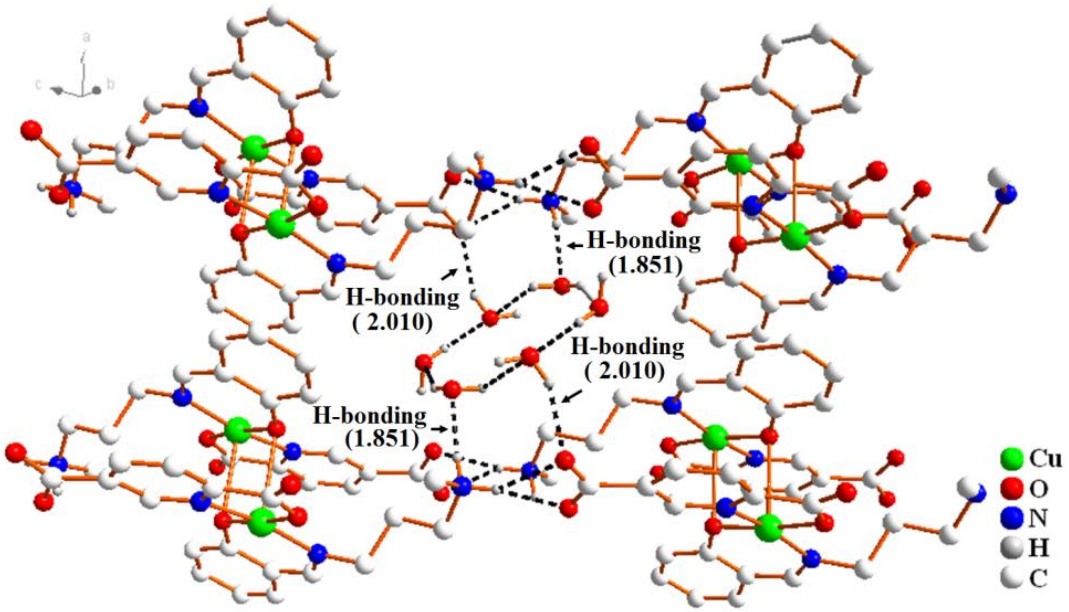

Fig. 5. 2D supramolecular structure of **2**.

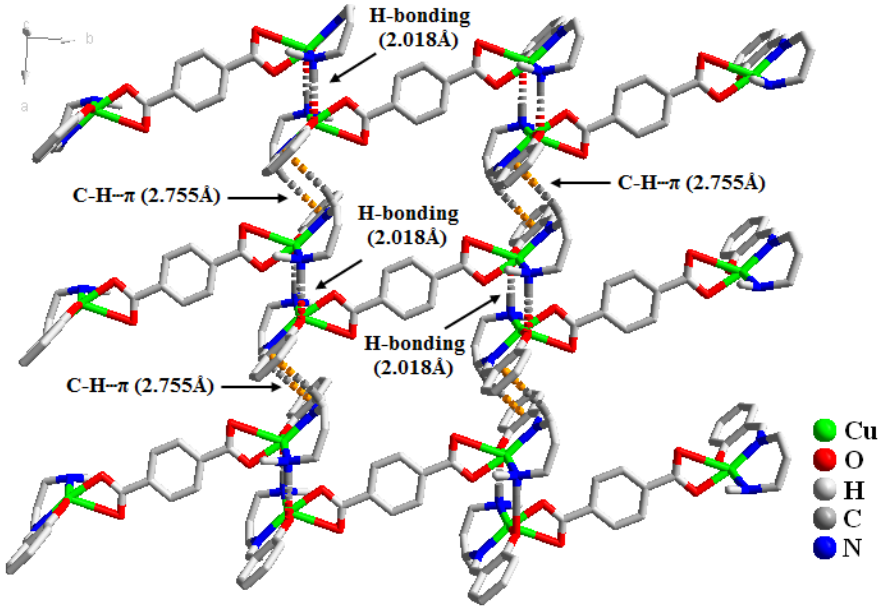

Fig. 6. 2D supramolecular structure of **3**.

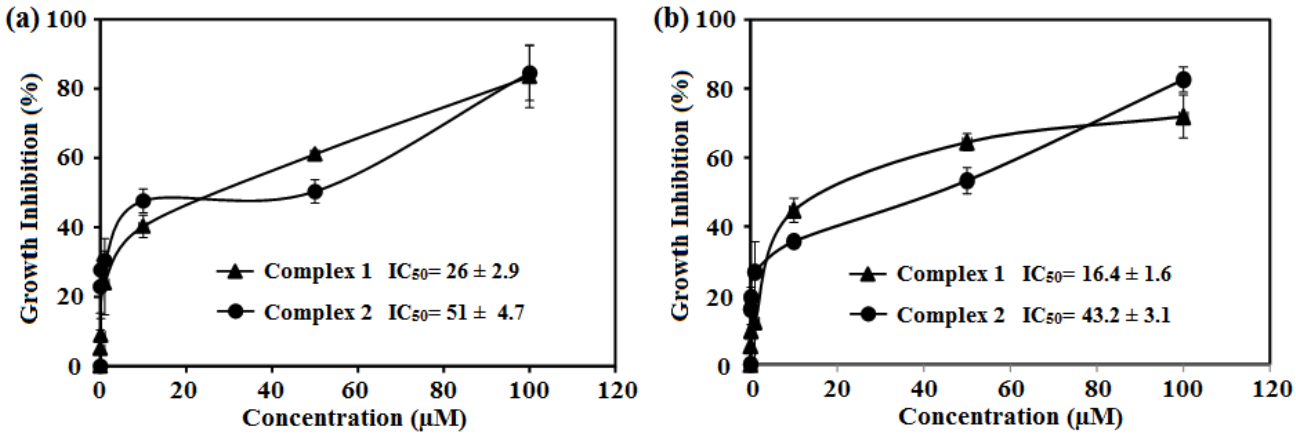

Fig. 7. The antiproliferative activity of **1** and **2** against human breast cancer cell lines (a) MCF7 and (b) MDA-MB-231. Cells were grown in the absence and presence of different concentrations of complex 1 and complex 2 for 48 h and then MTT assay was performed.

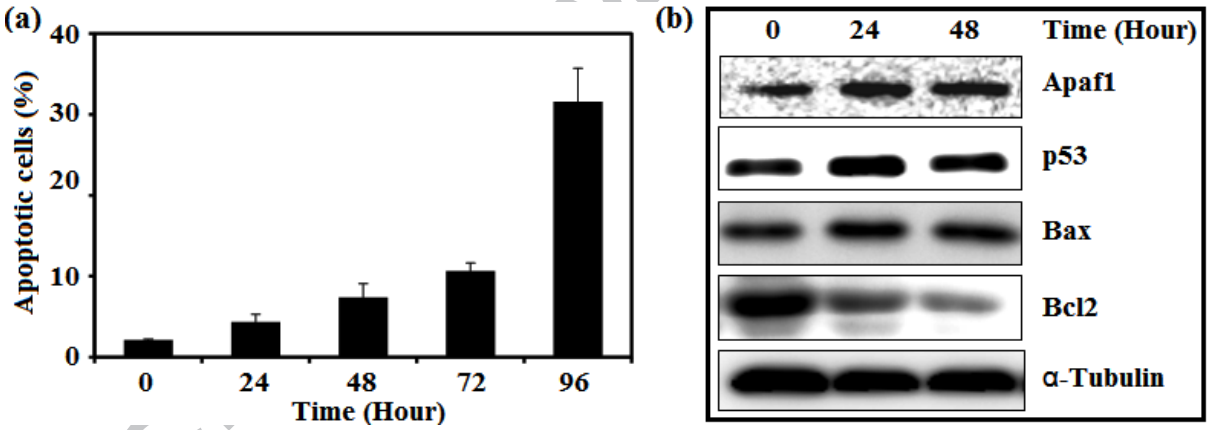

Fig. 8. (a) Potent cytotoxic activity of complex **1**, by FACS analysis.MDA-MB-231 cells were grown in the absence and presence of 25 μM of complex 1 for the indicated periods. Cells were then fixed, stained with PI and subjected to cell cycle profile analysis in FACS. **(b)** Complex **1** induces apoptosis. MDA-MB-231 cells were grown in the absence and presence of 25 μM of complex 1 for the indicated periods and whole cell protein extracts were immunoblotted for the indicated proteins.

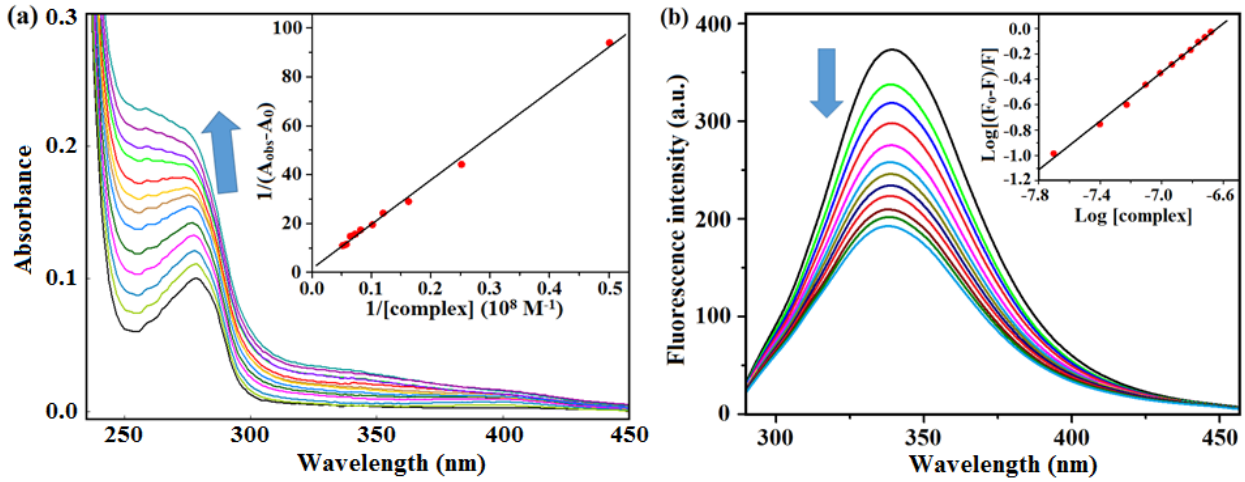

Fig. 9. (a) UV-vis absorption spectra of BSA (2 mL, 2.3 µM aqueous solution) upon gradual addition of 10µL 4µM aqueous solution of complex **1**. (b) Fluorescence spectra of BSA (2 mL, 6.2 µM) upon gradual addition of 10µL, 4µM aqueous solution of complex **1**.

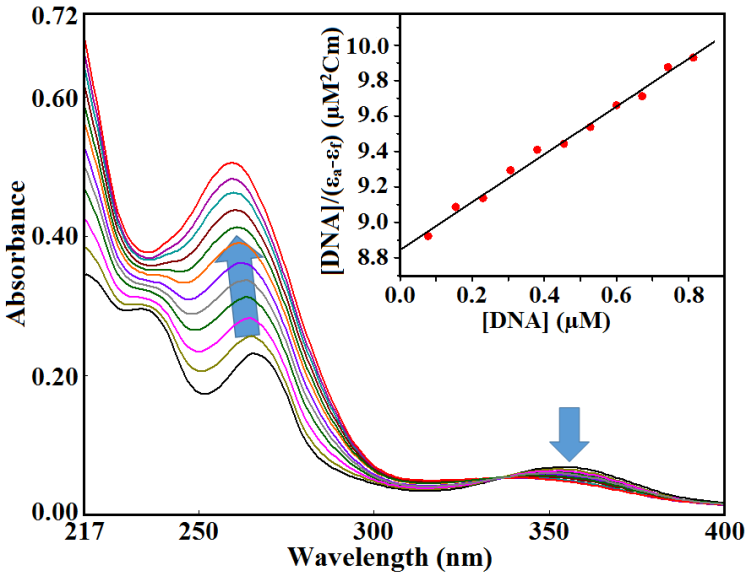

Fig. 10. Electronic absorption spectra of complex **1** (2 mL, 4µM) in HEPES buffer upon gradual addition of 10 µL, 15.6 µM aqueous solution of CT-DNA.

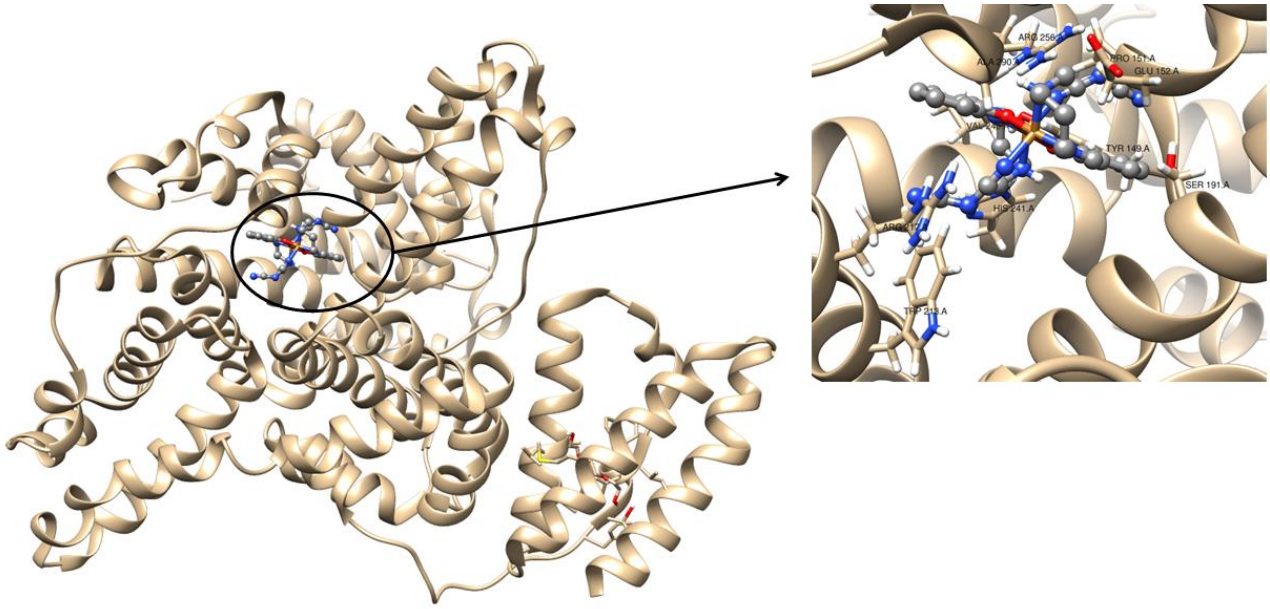

Fig. 11. Molecular docking image of **1** with BSA (binding site: *Tyr149*) showing binding sites.

Highlights

- Schiff base coordinated copper(II) complexes have been synthesized and characterized.
- Spectroscopic studies indicate complexes interact with serum albumin and CT-DNA.
- Molecular docking studies indicate interaction of complexes with serum albumins.
- Anticancer activities of complexes on MCF7 and MDA-MB- 231 cells have been performed.

For Table of Contents Use Only

Synthesis, crystal structure, cytotoxicity study, DNA / protein binding and molecular docking of dinuclear copper(II) complexes

Apurba Bhunia, Soumen Mistri, Manas Kumar Santra, Rajesh Kumar Manne, Subal Chandra Manna*

Dinuclear Cu(II) complexes have been synthesized and characterized by structure analyses. Cytotoxicity study reveals that complexes show dose dependent suppression of breast cells (MCF7 and MDA-MB- 231). Interactions of complexes with bovine serum albumin, human serum albumin and calf thymus DNA have been studied by electronic absorption and fluorescence spectroscopic techniques.